中国激光

2.3 W 双向抽运 3.5 μm 光纤激光器

张新[1]，佟存柱[1*]，蔡凯迪[1,2]，王延靖[1]，汪丽杰[1]，田思聪[1]

[1]中国科学院长春光学精密机械与物理研究所发光学及应用国家重点实验室，吉林 长春 130033；

[2]中国科学院大学材料科学与光电技术学院，北京 100049

摘要 功率低是限制中红外光纤激光器实际应用的一个关键因素，功率提升对于拓展其应用范围具有非常重要的意义。报道了 2 W 级近单模 3.5 μm 光纤激光实验装置，即采用 976 nm 和 1973 nm 两个波长的泵浦光源级联泵浦铒掺杂氟化物光纤(Er:ZBLAN)，实现了 3.5 μm 激光输出。为了进一步提升激光输出功率，采用双向抽运方法，最终实现的室温下连续输出的最高功率为 2.32 W。激光激射阈值约为 1.5 W，激光器工作时总的光光转换效率为 10.33%，中心波长为 3.54 μm，激光器工作模式为近单模，光束质量因子(M^2)小于 1.5。

关键词 激光器；中红外激光；光纤激光；双向泵浦；氟化物光纤

中图分类号 TN248.1 **文献标志码** A **DOI**：10.3788/CJL202249.1801001

1 引 言

近年来，随着中红外激光技术的不断发展，其在激光加工、红外对抗、气体检测以及激光医疗等领域中均显示出独特的优势[1-4]。尤其是 3.5 μm 光纤激光器更是凭借其良好的光束质量、高亮度以及处于大气透射窗口等特点而成为国内外的研究热点[5-8]。然而，传统方法是采用波长为 655 nm 的单个泵浦光源抽运 Er:ZBLAN 光纤以实现3.5 μm 激光输出[9]。但是，短波长泵浦光源易被激发态吸收而影响其转换效率，导致最终输出激光功率只有几个毫瓦。直到 2014 年，澳大利亚学者提出采用双波长级联泵浦的方式实现 3.5 μm 光纤激光激射，最高输出功率为 260 mW[10]。2015 年，加拿大学者采用光纤耦合器将双波长泵浦光合成一束，再将其耦合到 4.3 m 长的氟化物光纤中，将功率提升至 1.5 W[11]。2017 年，他们采用光纤光栅作为腔反馈镜，将功率刷新至 5.6 W[12]。2021 年，他们再次刷新纪录，实现的最高输出功率为 14.9 W，这是目前公开报道文献中 3.5 μm 波段连续输出的最高功率[13]。

国内在这方面的研究起步较晚，与国际水平还是有一定差距。2017 年，上海交通大学学者采用级联泵浦方式抽运掺杂浓度(摩尔分数)为 1.5% 的 Er:ZBLAN 光纤，将激射波长拓展到 3.68 μm，最高输出功率为 0.85 W[14]。2019 年，湖南大学学者为了减轻光纤端面散热压力，减小光路调节难度，将两个波长的泵浦光分别从光纤两端注入，最终实现了 1.72 W 的激光输出[15]。从其输出功率曲线可以看出，功率并没有饱和。因此，在保证光纤端面具有良好散热的基础上，将更大功率的 1973 nm 泵浦光源同时从光纤两端注入将会有助于进一步提升激光输出功率。

考虑到主要影响 3.5 μm 光纤激光功率提升的是 1973 nm 泵浦光源，本文采用两个自主研制的 1973 nm 泵浦光源，分别从光纤两端同时抽运，以提升其输出功率。对比单向抽运和双向抽运的激光输出功率，并测试了激光的输出光谱和光束质量。

2 实验装置

图 1(a)所示为双向抽运的 3.5 μm 光纤激光器的实验装置图。976 nm 泵浦光源采用的是光纤耦合半导体激光器，尾纤芯径和数值孔径分别为 105 μm 和 0.22。图 1(b) 是自主研制的 1973 nm 泵浦光源的结构示意图。采用 793 nm 光纤耦合半导体激光器作为泵浦光，将尾纤与光纤光栅(FBG)输入端熔接。光纤光栅的中心波长为 1973 nm，带宽为 2 nm，反射率约为 99%。输出端与 3 m 长铥掺杂石英光纤熔接，并且以光纤端面菲涅耳反射(反射率 $R=4\%$)作为输出。采用 45°双色镜 DM3[高反(HR)@1973 nm & 高透(HT)@793 nm]将产生的激光与残余泵浦光分离。图 1(c)是自制的 1973 nm 激光的输出功率曲线和转换效率，最高输出功率为 10 W，光光转换效率达到 53.8%。后向抽运(backward pumping)是通过 45°双

收稿日期：2021-11-12；**修回日期**：2021-12-21；**录用日期**：2022-01-17

基金项目：国家自然科学基金(61790584，61774153)、发光学及应用国家重点实验室自主课题(SKLA-Z-2021-07)、中国科学院青年创新促进会项目(2018249)

通信作者：*tongcz@ciomp.ac.cn

色镜 DM1(HR@1973 nm & HT@976 nm),将自制 1973 nm 泵浦光源 P1 与 976 nm 泵浦光源合成一束,并采用非球面聚焦透镜 L2 将其耦合到 Er:ZBLAN 光纤。光纤长度为 4.8 m,掺杂浓度(摩尔分数)为 1%,纤芯直径和数值孔径分别为 17.8 μm 和 0.12,包层直径和数值孔径分别为 250 μm 和 0.5。光纤两端均切成 0°角,并且与腔镜紧密贴合。L1~L4 为硒化锌(ZnSe)非球面透镜,焦距均为 12.7 mm。L5 为石英非球面镜,焦距为 8 mm。输出耦合镜的反射率约为 60% @ 3500 nm(HT @ 1973 nm & HT @ 976 nm),3.5 μm 激光通过 45°双色镜 DM2(HR@3500 nm & HT@1973 nm &HT@976 nm)从系统中输出。前向抽运(forward pumping)是从光纤另一端耦合另一个自制的 1973 nm 泵浦光源 P2。测试系统有中红外功率计、中红外傅里叶光谱仪和光束质量分析仪。

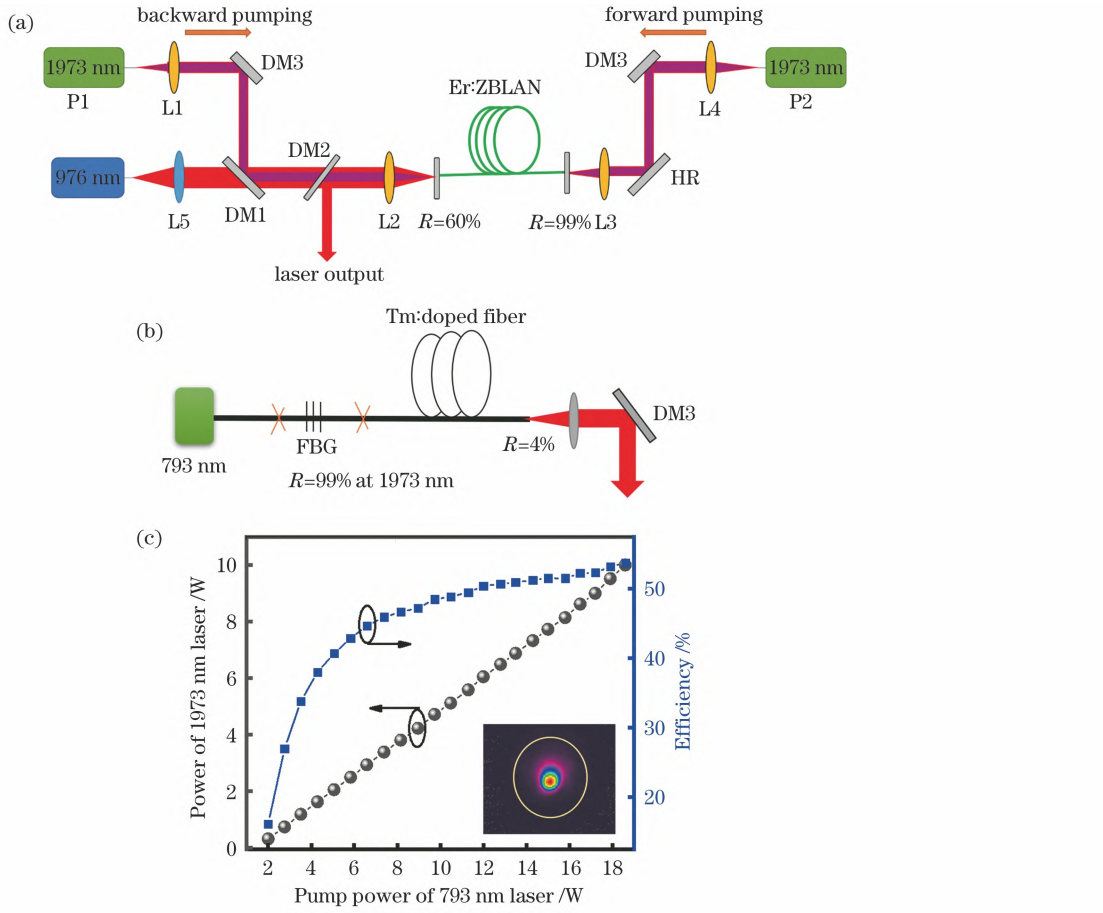

图 1　实验装置示意图及 1973 nm 泵浦光功率和转换效率曲线。(a)双向抽运 3.5 μm 光纤激光器的实验装置图;(b) 自制的 1973 nm 泵浦光源的结构示意图;(c) 自制的 1973 nm 激光的输出功率和转换效率曲线

Fig. 1 Schematics of experimental setup and power and conversion efficiency curves of homemade 1973 nm laser. (a) Experimental setup for bidirectional pumping of 3.5 μm fiber laser; (b) schematic of homemade 1973 nm pump light source; (c) output power and conversion efficiency curves of homemade 1973 nm laser

3　实验结果与分析

首先分别实现了后向和前向抽运下的激光激射,图 2 所示为单向抽运激光的输出功率曲线。可以看出,后向抽运下激光器的输出功率要比前向抽运略微高一些。后向抽运时,976 nm 和 1973 nm 两个泵浦光源均从光纤同一端注入,沿着光传输方向的功率分布一致,即在 976 nm 泵浦光功率高的地方,对应的 1973 nm 泵浦光功率也高,所以激光转换效率要高于前向抽运,对应的激光输出功率也会比前向抽运高。当固定 976 nm 泵浦光的功率时,输出激光功率先是随着 1973 nm 泵浦光功率的增加而增大,然后达到饱和。而此时如果增加 976 nm 泵浦光功率,输出功率将会继续随 1973 nm 泵浦光功率的增加而增大。其原因可以根据 3.5 μm Er:ZBLAN 光纤激光能级结构进行分析,如图 3 所示。976 nm 泵浦光将基态粒子抽运到 $^4I_{11/2}$ 能级上,1973 nm 泵浦光再将 $^4I_{11/2}$ 能级上的粒子抽运到上能级,从而实现 3.5 μm 激光激射。而当 976 nm 泵浦光功率较低时,抽运到 $^4I_{11/2}$ 能级的粒子数较少,不满足 1973 nm 泵浦光抽运的需求,则出现激光输出功率饱和。此时,如果增加 976 nm 泵浦光功率,即增加 $^4I_{11/2}$ 能级的粒子数,输出激光会继续随着 1973 nm 泵浦光功率的增加而增大。当然 976 nm泵浦光功率也不宜过高,抽运到 $^4I_{11/2}$ 能级的

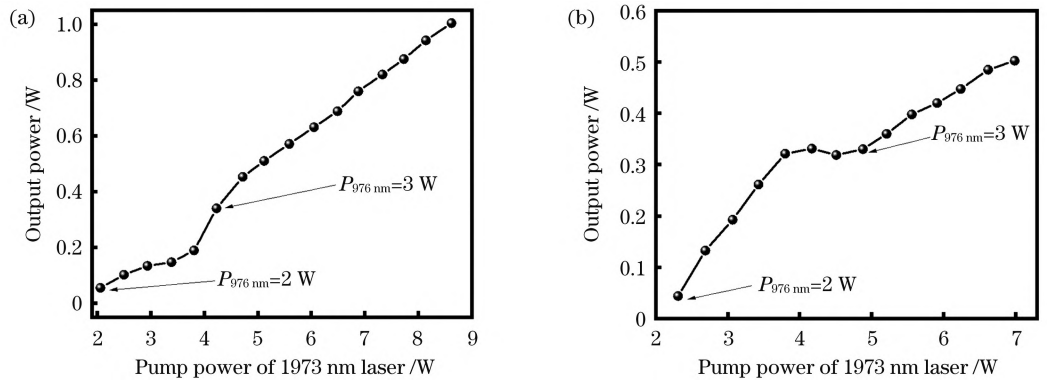

图 2　单向抽运 3.5 μm 光纤激光器的输出功率曲线。(a)后向抽运;(b)前向抽运

Fig. 2　Output power curves of 3.5 μm fiber laser by unidirectional pumping. (a) Backward pumping; (b) forward pumping

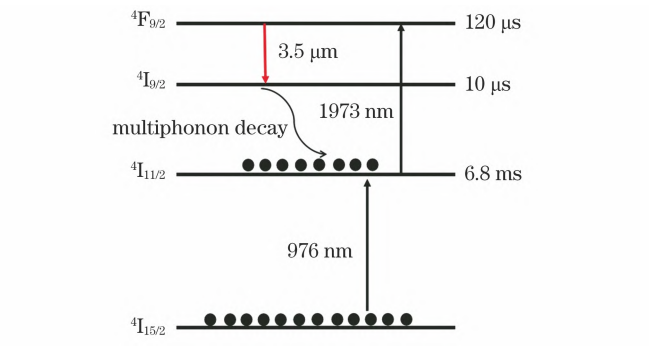

图 3　3.5 μm Er∶ZBLAN 光纤激光的能级结构

Fig. 3　Energy levels of 3.5 μm Er∶ZBLAN fiber laser

粒子数与1973 nm 泵浦光匹配即可,否则 976 nm 泵浦光功率过高,不仅不会提升输出激光功率,反而会增加光纤端面散热压力。

在充分优化前向和后向抽运激光输出功率的基础上,开展双向抽运实验。先是开启后向抽运,在其达到最大输出功率时,再开启前向抽运。随着 1973 nm 泵浦光功率的不断增加,976 nm 泵浦光功率也需相应增加。其功率曲线如图 4 所示,当 1973 nm 泵浦光功率超过 1.5 W 时,激光开始激射,最终实现最高输出功率 2.32 W,激光工作时总的光光转换效率为 10.33%。

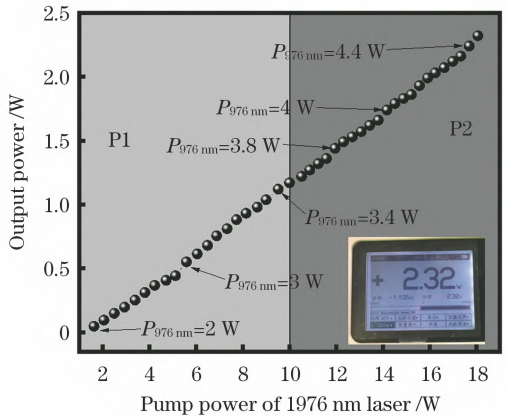

图 4　双向抽运 3.5 μm 光纤激光器的输出功率曲线

Fig. 4　Output power curve of 3.5 μm fiber laser by bidirectional pumping

采用中红外傅里叶光谱仪测试 3.5 μm 光纤激光在不同泵浦功率下的输出光谱,结果如图 5 所示。当1973 nm 泵浦光功率为 2 W 时,激射光谱中心波长为3457 nm。当泵浦功率大于 2 W 时,激光中心波长由3457 nm 变为 3539 nm,波长大幅度变化是因为增加泵浦功率时,$^4I_{9/2}$ 能级会积累大量粒子,这些粒子无法尽快清空,从而导致上能级跃迁下来的粒子会跃迁到高于 $^4I_{9/2}$ 能级的亚能级上,进而导致波长向长波方向发生转变[14-15]。继续增加泵浦功率,中心波长只有微弱的红移。

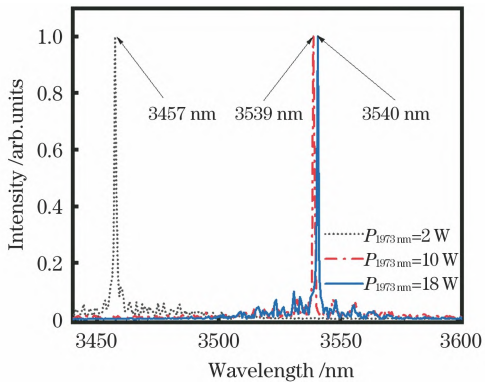

图 5　不同泵浦功率下 3.5 μm 光纤激光的输出光谱

Fig. 5　Output spectra of 3.5 μm fiber laser under different pump powers

利用热释电相机采集 3.5 μm 激光输出光斑包络和光斑直径。依据激光光束质量测试方法计算激光光束质量因子(M^2),其结果如图 6 所示。激光光斑整体为基模形态,光束质量因子 M^2 小于 1.5。

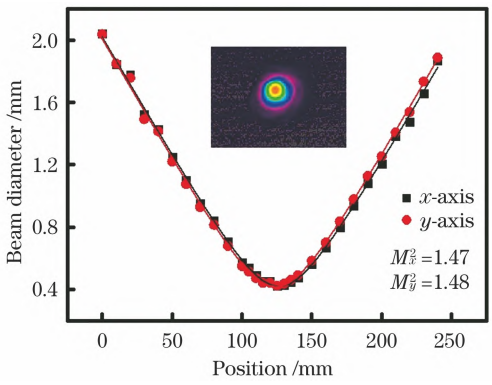

图 6　3.5 μm 光纤激光器的光束质量及其输出光斑包络

Fig. 6　Beam quality and output beam profile of 3.5 μm fiber laser

同时，我们也从理论上分析双向抽运的优势。根据 Malouf 等[16]建立的级联泵浦模型，理论分析对比了单向抽运和双向抽运 3.5 μm 光纤激光器腔内各波长激光的功率变化情况，结果如图 7(a)、(c) 所示。单向抽运对应的 1973 nm 泵浦功率设置为 18 W，双向抽运对应的两端 1973 nm 泵浦功率分别设置为 10 W 和 8 W。可以看出，双向抽运泵浦光几乎完全被吸收，对应的腔内 3.5 μm 激光功率比单向抽运高。采用 Ashoori 等[17]构建的氟化物光纤热分析模型，理论分析了单向抽运和双向抽运方式下光纤的轴向热量分布，结果如图 7(b)、(d)所示。在相同泵浦功率下，单向抽运方式下泵浦端的最高温度达到 490 K，光纤内的最大温差大约为 170 K，而双向抽运方式下泵浦端的最高温度为 416 K，光纤内的最大温差大约为 50 K。双向抽运可以匀化光纤内部的能量分布，减小光纤端面的散热压力，是提升该波段激光功率的一种有效方法。

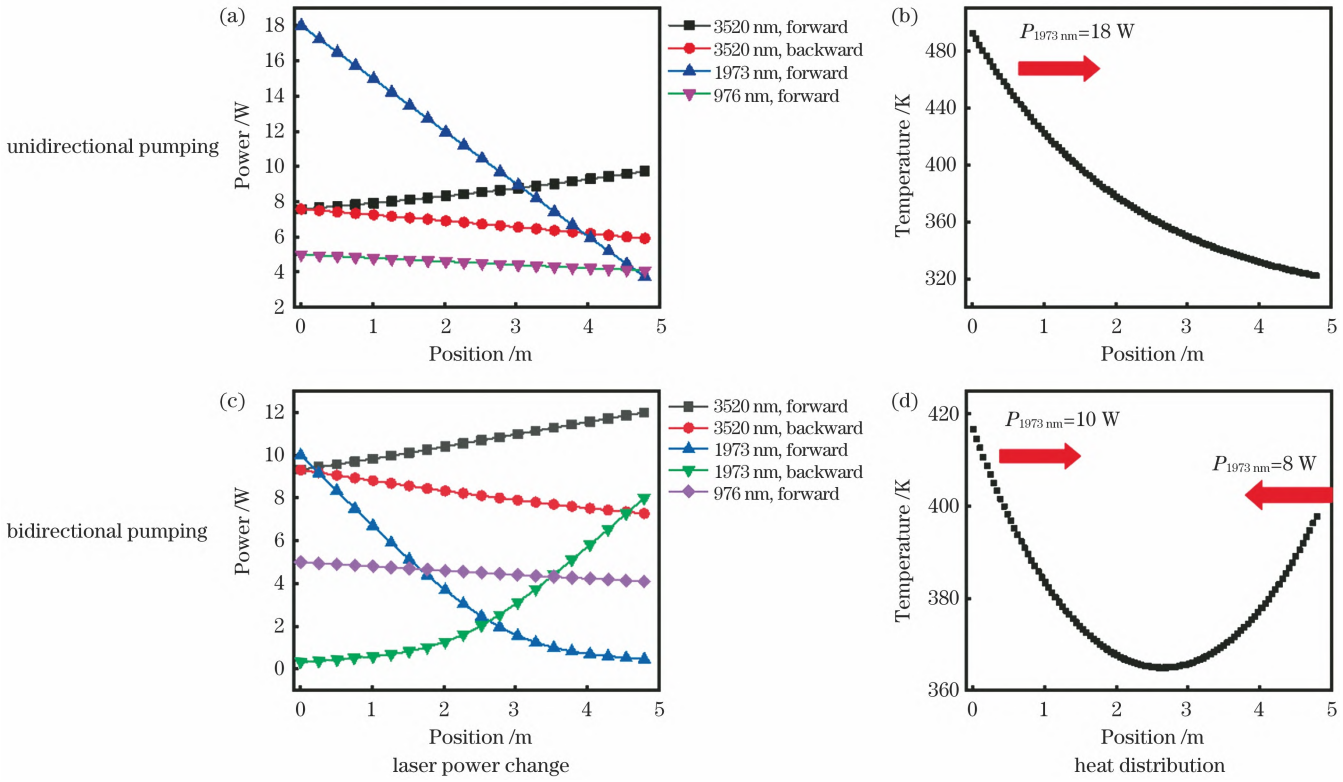

图 7　不同抽运方式下 3.5 μm 光纤激光器腔内各个波长激光的功率变化和热量分布

Fig. 7　Power change of each wavelength laser in 3.5 μm fiber laser cavity and heat distribution under different pumping schemes

4　结　　论

基于自制的 1973 nm 泵浦光源，通过双向抽运铒掺杂氟化物光纤 Er∶ZBLAN，实现了室温下高功率近单模 3.5 μm 激光的连续输出。最大输出功率为 2.32 W，激光工作时总的光光转换效率为 10.33%。在最大抽运功率下，光纤端面没有出现损伤。当泵浦功率较低时，输出激光的中心波长为 3457 nm，当泵浦功率增加时，中心波长变为 3540 nm。激光光斑整体为基模形态，光束质量因子 M^2 小于 1.5。通过优化抽运结构及光纤参数，还可以进一步提升 3.5 μm 光纤激光功率。

参　考　文　献

[1] Sorokina I T, Vodopyanov K L. Solid-state mid-infrared laser sources[M]. Heidelberg: Springer, 2003.

[2] Mahon R, Burris H R, Ferraro M S, et al. A comparative study of 3.6 μm and 1.55 μm atmospheric transmission [J]. Proceedings of SPIE, 2008, 6951: 69510Q.

[3] 杨俊彦, 公发全, 刘锐, 等. 中红外激光在光电对抗领域的应用及进展[J]. 飞控与探测, 2020, 3(6): 34-42.
Yang J Y, Gong F Q, Liu R, et al. Application and progress of mid-infrared laser in optoelectronic countermeasure field [J]. Flight Control & Detection, 2020, 3(6): 34-42.

[4] 江健涛, 魏蒙恩, 熊正东, 等. 子脉冲序列模式 Er∶YAG 激光消融牙本质的实验观察[J]. 中国激光, 2021, 48(1): 0107001.
Jiang J T, Wei M E, Xiong Z D, et al. Observation of dentin ablation using an Er∶YAG laser in a sub-pulse sequence mode [J]. Chinese Journal of Lasers, 2021, 48(1): 0107001.

[5] Bawden N, Matsukuma H, Henderson-Sapir O, et al. Actively Q-switched dual-wavelength pumped Er^{3+}∶ZBLAN fiber laser at 3.47 μm[J]. Optics Letters, 2018, 43(11): 2724-2727.

[6] Jobin F, Fortin V, Maes F, et al. Gain-switched fiber laser at 3.55 μm[J]. Optics Letters, 2018, 43(8): 1770-1773.

[7] Luo H Y, Yang J, Liu F, et al. Watt-level gain-switched fiber laser at 3.46 μm[J]. Optics Express, 2019, 27(2): 1367-1375.

[8] Wei J C, Li P, Yu L P, et al. Mode-locked fiber laser of 3.5 μm using a single-walled carbon nanotube saturable absorber mirror [J]. Chinese Optics Letters, 2022, 20(1): 011404.

[9] To bben H. Room temperature cw fibre laser at 3.5 μm in Er^{3+}-doped ZBLAN glass [J]. Electronics Letters, 1992, 28 (14): 1361-1362.

[10] Henderson-Sapir O, Munch J, Ottaway D J. Mid-infrared fiber lasers at and beyond 3.5 μm using dual-wavelength pumping[J]. Optics Letters, 2014, 39(3): 493-496.

[11] Fortin V, Maes F, Bernier M, et al. Watt-level erbium-doped all-fiber laser at 3.44 μm[J]. Optics Letters, 2016, 41(3): 559-562.
[12] Maes F, Fortin V, Bernier M, et al. 5.6 W monolithic fiber laser at 3.55 μm[J]. Optics Letters, 2017, 42(11): 2054-2057.
[13] Lemieux-Tanguay M, Fortin V, Boilard T, et al. 15 W all-fiber laser at 3.55 μm[J]. Optics Letters, 2022, 47(2): 289-292.
[14] Qin Z P, Xie G Q, Ma J G, et al. Mid-infrared Er∶ZBLAN fiber laser reaching 3.68 μm wavelength[J]. Chinese Optics Letters, 2017, 15(11): 111402.
[15] Zhang C X, Wu J D, Tang P H, et al. ~3.5 μm Er^{3+}∶ZBLAN fiber laser in dual-end pumping regime[J]. IEEE Access, 2019, 7: 147238-147243.
[16] Malouf A, Henderson-Sapir O, Gorjan M, et al. Numerical modeling of 3.5 μm dual-wavelength pumped erbium-doped mid-infrared fiber lasers[J]. IEEE Journal of Quantum Electronics, 2016, 52(11): 16332584.
[17] Ashoori V, Malakzadeh A. Explicit exact three-dimensional analytical temperature distribution in passively and actively cooled high-power fibre lasers[J]. Journal of Physics D: Applied Physics, 2011, 44(35): 355103.

2.3 W 3.5 μm Fiber Laser Based on Bidirectional Pumping

Zhang Xin[1], Tong Cunzhu[1*], Cai Kaidi[1,2], Wang Yanjing[1], Wang Lijie[1], Tian Sicong[1]

[1] *State Key Laboratory of Luminescence and Applications, Changchun Institute of Optics, Fine Mechanics and Physics, Chinese Academy of Sciences, Changchun* 130033, *Jilin, China*;

[2] *College of Materials Science and Opto-Electronic Technology, University of Chinese Academy of Science, Beijing* 100049, *China*

Abstract

Objective There is an increasing scientific interest in developing mid-infrared laser sources to fulfill various application requirements in the biomedical, defense and security, and material processing. In particular, the 3.5 μm fiber laser has become a research hotspot due to its good beam quality, high brightness, and being in an atmospheric window. Limited by the nature of fiber materials and lack of fiber optical devices, the power of a mid-infrared fiber laser is two to three orders of magnitude less than that of a near-infrared laser. However, the low power of a mid-infrared fiber laser is a key factor limiting its practical applications. It is great significance for expanding its application fields to improve the power of a mid-infrared fiber laser.

Methods The method of cascade pumping is proposed to achieve a high efficiency 3.5 μm fiber laser. The 1973 nm and 976 nm dual-wavelength laser source is used to pump the Er-doped fluoride fiber (Er∶ZBLAN). The ground-state particles are pumped by the 976 nm laser to the energy level of $^4I_{11/2}$, and the particles at the $^4I_{11/2}$ energy level are pumped by the 1973 nm laser to the upper energy level to achieve a 3.5 μm laser. However, the end of a fiber would be damaged under a high pump power. Considering that the main factor of the 3.5 μm laser power is the 1973 nm pump power, the bidirectional pumping scheme is proposed to improve the output power here. Double homemade 1973 nm pump laser sources are coupled into the 4.8 m long Er∶ZBLAN fiber. The core diameter and numerical aperture of the fiber are 17.8 μm and 0.12, the cladding diameter and numerical aperture are 250 μm and 0.5, and the doping concentration (mole fraction) is 1%. Both ends of the optical fiber are cut into a 0° angle and closely attached to the cavity mirror. The reflectivity of the output coupling mirror is about 60% at 3500 nm (high transmission @1973 nm & high transmission @976 nm). And a 45° dichroic mirror DM2 (high reflection @ 3500 nm & high transmission @ 1973 nm & high transmission @976 nm) is used to output a 3.5 μm laser from the system.

Results and Discussions First, the 3.5 μm lasers are realized by forward and backward pumping, respectively. And the output powers are measured (Fig. 2). It can be seen that the output power for backward pumping is slightly higher than that for forward pumping. When the 976 nm pump power is fixed, the output power increases with the increase of the 1973 nm power and then reaches saturation. At this time, the output power continues to increase with the increase of the 1973 nm pump power when the 976 nm pump power increases. The reason can be analyzed by the energy level structure of the 3.5 μm Er∶ZBLAN fiber laser (Fig. 3). The ground-state particles are pumped by the 976 nm laser to the energy level of $^4I_{11/2}$ and subsequently these particles are pumped by the 1973 nm laser to the upper energy level to achieve a 3.5 μm laser. When the 976 nm pump power is low, the number of particles at the $^4I_{11/2}$ energy level is small. The output laser power will be saturated under the high 1973 nm pump power. And the output power continues to increase with the increase of the 1973 nm pump power by enhancing the 976 nm pump power, because the number of particles at the $^4I_{11/2}$ energy level increases under the high 976 nm pump power. Of course, the number of particles pumped to the $^4I_{11/2}$ energy level should be matched with the 1973 nm pump power. The excessively high 976 nm pump power would not contribute to improve the laser power, but increase the heat dissipation pressure on the fiber end face. By fully optimizing the 3.5 μm laser output power in both forward and backward pumping, the bidirectional pumping is conducted. When the backward pumping is turned on and the maximum output power is realized, the forward pumping is then turned on. With

the increase of the 1973 nm pump power, the 976 nm power is also increased complementarily. The power curve for bidirectional pumping is recorded (Fig. 4). The laser threshold is 1.5 W, the maximum output power is 2.32 W, and the total light-to-light conversion efficiency is 10.33%. The output spectra under different pump powers are measured by the mid-infrared Fourier spectrometer (Fig. 5). When the 1973 nm pump power is 2 W, the central wavelength of the lasing spectrum is 3457 nm. As the pump power exceeds 2 W, the central wavelength is switched to 3539 nm. The beam envelope and diameter of the 3.5 μm output laser are measured by pyroelectric camera. The beam quality factor (M^2) is calculated according to the laser beam quality test method (Fig. 6). The output laser beam presents a fundamental mode Gaussian distribution and its beam quality factor M^2 is less than 1.5.

Conclusions Based on the homemade 1973 nm pump sources, a 3.5 μm Er∶ZBLAN fiber laser based on bidirectional pumping is achieved at room temperature. The maximum output power is 2.32 W, and the total light-to-light conversion efficiency is 10.33%. And there is no damage on the fiber end under the maximum pump power. When the 1973 nm pump power is below 2 W, the laser central wavelength is 3457 nm. The central wavelength is switched to 3540 nm as the 1973 nm pump power exceeds 2 W. The envelope of the laser beam presents a fundamental mode Gaussian distribution and the beam quality factor M^2 is less than 1.5. By optimizing the pumping structure and fiber parameters, the laser power can be further improved.

Key words lasers; mid-infrared laser; fiber laser; bidirectional pumping; fluoride fiber